Proceedings of the Korean Nuclear **Society** Spring Meeting
Gyeongju, Korea, 2004

Liquid Droplet Deformation in Non-wetted and Wetted Surface during Impingement

Shane Park, Gyoo Dong Jeun

Hanyang University
17 Haengdang, Sungdong
Seoul, Korea 133-791

Song Hyo Bae

Korea Institute of Science and Technology Evaluation and Planning
275 Yangjae, Seocho
Seoul, Korea 137-130

Abstract

Analytical study of water droplet deformation when the droplet impinged onto wetted and non-wetted solid surface is calculated. This analytical work is performed by the Moving Particle Semi-implicit(MPS) method which solves the unsteady Navier-Stokes equations for the liquid droplets. Accurate analysis of the liquid droplet interacting with a solid surface will provide an essential input to understand the dynamic process of droplet impingement which encounters in spray cooling process in many industrial processes. One of important application is also in the analysis of reflooding process of LOCA in nuclear reactor. The present work is, however, limited to an adiabatic process, i.e., no heat transfer between the liquid droplet and solid surface. However, hydrodynamic aspects of the liquid droplet deformation during the impingement are still essential to investigate the subsequent heat transfer during the process.

1. Introduction

Quenching of a heated surface commonly encounters in many physical processes which involves the interaction between a coolant and a heated medium, such as boiling systems, cryogenic systems, metallurgical processing, and steam generators. This phenomenon is also an essential issue in the assurance and reduction of safety margins in many boiling systems

which include nuclear reactors.

In nuclear reactor, the design of the nuclear reactor is based on a hypothetical accident scenario, so-called LOCA(Loss-Of-Coolant Accidents), in which the nuclear core with continuous residual heat generation due to the decay heat of nuclear fuel even after the reactor shutdown can be overheated by the loss of coolant. For safe design of the reactors, the continuous overheating of fuel rods without adequate cooling which may eventually cause catastrophic core melting should be prevented. The adequate cooling during LOCAs is provided by the Emergency Core Cooling System(ECCS). The cold water to cool the overheated core is introduced into the Reactor Pressurized Vessel(RPV) during the reflooding phase of the accidents. During this phase the reflooding of coolant into the overheated core, however, violent boiling processes occur. Therefore, the adequate evaluation of the safety margin in relation to the peak temperature of the overheated fuel rods, or peak cladding temperature(PCT) during the hypothetical LOCA is largely connected to an accurate prediction of the cooling of the cladding during the reflooding phase.

In fact, reflooding process involves a variety of basic flow phenomena(bottom and top quench, droplet formation, droplet break-up, droplet de-entrainment, grid effects, etc.) which also affect the cooling process at various scales. Reflooding is characterized by a multiplicity of scales and basic phenomena, including:

- System scale(coupling between core and loops)
  - ✓ Oscillatory flow, steam binding, core inlet flow, radial mixing, pool formation, etc.
- Macro scale(homogeneous portions of the core, subassembly)
  - ✓ Entrainment, quench front propagation, etc.
- Meso scale(subchannel scale)
  - ✓ Heat transfer modes, droplet formation, evolution and distribution, etc.
- Micro scale(droplet scale or film scale)
  - ✓ Details of liquid-wall interaction and rewetting

The predictive capabilities of current analysis tools are reasonable for a broad range of conditions but are far from being universal. In fact, they often fail to simulate tests with geometries(e.g., tight lattice) and conditions(high initial temperatures as a consequence of limited emergency core cooling availability), substantially different from those included in the database used during the development of their models. Simulation tools are essentially one-dimension and extensions of the models to three-dimension in a porous body approach are available in some system codes, e.g., TRAC, which can only account for large-scale three-dimensional effects.

Computational Fluid Dynamics(CFD) codes have not been used yet for the analysis of this phenomenology, but they have potential with respect to two different areas of application. Firstly, they can provide a more accurate calculation of distribution effects without resort to empirical approaches. Secondly, recent successes in calculating steady-state void fraction distributions in complex geometries(including multi-field formulations of interactions of annular-dispersed flows with obstacles) should encourage their use in analyzing a number of

processes at the appropriate scale, especially for developing more accurate closure laws for more global approaches. At present, however, due to computer power limitations and basic difficulties(practical as well as theoretical) to include all the small-scale processes in a full-scale transient simulation, the use of CFD for global reflooding modeling cannot be envisaged.

Recent advances of the CFD techniques in the interface tracking between two phases, such as, liquid and vapor enable directly to simulate various multiphase flow and heat transfer phenomena. This numerical investigation allows investigating the detail multiphase phenomena such as liquid droplet entrainment and detrainment during the reflooding phases. There are a number of techniques, such as the Level set method, the Volume of Fluid(VOF) method, the CIP(Cubic interpolated Propagation) method, Lattice Boltzmann method, Moving Particle Semi-implcit(MPS) method, etc.

During the reflooding phase of the LOCA accident, accurate prediction of the droplet entrainment and detrainment in the reflooding coolant and the post-dryout heat transfer in the downstream of the reflooding coolant is of essence to evaluate the peak cladding temperature of the fuel. First, in the post-dryout region, the main heat transfer mode will be the quenching process due to the small-scale liquid droplets in the mist flow on the heated fuel rod surface. To understand this type of quenching process, the interaction between the solid surface and liquid droplet will be of importance. When the misty liquid droplet impinges on the heated surface, the deformation of the liquid droplet will provide impinges on the heated surface, the deformation of the liquid droplet will provide the interfacial area to transfer energy from the surface to the droplet.

Second, the distribution of liquid in the mist flow during the reflooding of coolant is determined by a mass balance between the liquid droplet generation from the reflooding coolant and the liquid droplet detrainment to the reflooding coolant when quenching front progresses. Therefore the investigation of the microscopic droplet entrainment and detrainment phenomenon with a single liquid droplet will be of essential.

In this work, the micro-scale phenomena during the reflooding of coolant, such as droplet impingement on the non-wetted solid surface and wetted solid surface which cover the phenomena mentioned in the previous paragraphs such as quenching of the heated fuel rod by a liquid droplet and liquid droplet detrainment, will be investigated.

The present work is limited to investigate the adiabatic case or hydrodynamic aspect of the phenomena. However, hydrodynamic aspects of the liquid drop deformation during the impingement are still essential to investigate the subsequent heat transfer during the process. The work will also continue to investigate the quenching phenomena by the improvement of out CFD codes with consideration of an adequate energy equation.

In addition, this analysis will give invaluable information in many other applications, such as spray cooling, fuel injection in the engine combustion, condenser and boilers, as well as the micro-ink jet and micro-system cooling devices, etc.

2. Analytical Method

2.1 General Navier-Stokes Equations

Governing equations are the mass and momentum conservation equations:

$$\frac{D\rho}{Dt} = 0 . \tag{1}$$

$$\rho \frac{D\boldsymbol{u}}{Dt} = -\nabla P + \mu \nabla^2 \boldsymbol{u} + \rho g + \sigma \kappa \delta \boldsymbol{n} . \tag{2}$$

where D/Dt denotes the Lagrangian derivative involving advection terms, $\boldsymbol{u}$ is the fluid velocity, P is the fluid pressure, ρ and μ are the density and viscosity, respectively, σ is the interfacial tension coefficient, κ is the mean curvature of interface, $\delta(s)$ is Dirac delta function concentrated on the interface, $\boldsymbol{n}_s$ is the unit normal vector to the interface.

2.2 Moving Particle Semi-Implicit Method

2.2.1 Particle Interaction Models

In the MPS method, particle interaction models are prepared for the differential operators. All the interactions are limited to neighboring particles covered with a weight function:

$$w(r) = \begin{cases} \dfrac{r_e}{r} - 1 & 0 \le r \le r \\ 0 & r_e \le r \end{cases}, \tag{3}$$

Where r_e is the radius of the interaction area, r_e =2.1l_0 in this study, l_0 represents the distance between adjacent particles in the initial arrangement and r is the distance between two particles. The weight function is zero when r is longer than r_e.

Summation of the weight function is called particle number density, which is used as a normalization for averaging.

$$n_i = \sum_{j \ne i} w\left(\left|\boldsymbol{r}_j - \boldsymbol{r}_i\right|\right). \tag{4}$$

The particle number density is proportional to the fluid density. It should be constant for incompressible flows: n_i=n_0, where n_0 is dependent on the initial arrangement of particles.

Gradient and Laplacian operators involved in the governing equations are transformed to equivalent particle interactions. If ϕ is an arbitrary scalar, particle interaction models for differential operators are expressed as

$$\left\langle \nabla \phi \right\rangle_i = \frac{d}{n^0} \sum_{j \ne i} \frac{\phi_j - \phi_i}{\left|\boldsymbol{r}_j - \boldsymbol{r}_i\right|^2} \left(\boldsymbol{r}_j - \boldsymbol{r}_i\right) w\left(\left|\boldsymbol{r}_j - \boldsymbol{r}_i\right|\right), \tag{5}$$

$$\left\langle \nabla^2 \phi \right\rangle_i = \frac{2d}{\lambda_i n^0} \sum_{j \ne i} \left(\phi_j - \phi_i\right) w\left(\left|\boldsymbol{r}_j - \boldsymbol{r}_i\right|\right), \tag{6}$$

Where d is the number of space dimensions and λ_i is defined as

$$\lambda_i = \frac{\sum_{j \neq i} \left| \boldsymbol{r}_j - \boldsymbol{r}_i \right|^2 w\left(\left| \boldsymbol{r}_j - \boldsymbol{r}_i \right| \right)}{\sum_{j \neq i} w\left(\left| \boldsymbol{r}_j - \boldsymbol{r}_i \right| \right)}. \tag{7}$$

The gradient model is obtained as the average of gradient vectors, which are determined between particle *i* and its neighboring particles *j*. The Laplacian model is derived from the physical concept of diffusion. The parameter λ_i is introduced to make the variance increase equal to that of the analytical solution.

Substituting the above particle interaction models into the governing equations, we can obtain the particle dynamics to simulate fluid flows. More details are described in Koshizuka and Oka(1996).

2.2.2 Computational Algorithm

A semi-implicit algorithm is used for incompressible flows in the MPS method. For incompressible flows, the continuity equation requires the fluid density to be constant. This is equivalent to the particle number density n_i being constant. In each time step, the governing equations are calculated through two steps.

In the first step, all terms in the momentum conservation equation except the pressure gradient term are explicitly calculated and temporal velocities and positions of particles are obtained:

$$\boldsymbol{u}_i^* = \boldsymbol{u}_i^n + \Delta t \left(\frac{\mu \nabla^2 \boldsymbol{u}^n + \sigma \kappa \delta(s) \boldsymbol{n}_s}{\rho_i} + g \right), \tag{8}$$

$$\boldsymbol{r}_i^* = \boldsymbol{r}_i^n + \Delta t \cdot \boldsymbol{u}_i^*, \tag{9}$$

Where μ is the kinematic viscosity. At this moment, the incompressibility constraint may not be satisfied, that is to say, the temporal particle number density n^* is not n^0. The temporal value n^* is implicitly corrected to n^0 by

$$n' = n^0 - n^*, \tag{10}$$

Where *n*' is the correction value. This is related to the velocity correction *u*' through the mass conservation equation:

$$\frac{1}{\Delta t} \frac{n'}{n^0} = -\nabla \cdot u'. \tag{11}$$

The velocity correction is derived from the implicit pressure gradient term as

$$u' = -\frac{\Delta t}{\rho} \nabla P^{n+1}. \tag{12}$$

With Eqs. (10)-(12), a Poisson equation for pressure is obtained:

$$\left\langle \nabla^2 P^{n+1} \right\rangle_i = -\frac{\rho}{\Delta t^2} \frac{n_i^* - n^0}{n^0}. \tag{13}$$

In the second step, the above Poisson equation for pressure is solved. Substituting the

present Laplacian model to the left side of Eq. (13), we obtain a set of symmetric linear equations, which can be solved by the incomplete Cholesky decomposition conjugate gradient(ICCG) method. The pressure gradient term is then calculated and the velocities and the positions of particles are modified.

2.2.3 Surface tension model

The particles that satisfy the following condition are regarded as on the interface:

$$n_i < \beta n^0 . \tag{14}$$

where, β is a parameter and 0.97 is employed in this study. The calculation result is not sensitive to the value of β as reported in Ref. ?.

The surface tension model(Nomura et al., 2001) is shown in Fig. 1. The curvature κ and the unit normal vectors n of the interfacial particles are calculated based on particle number density. Surface tension is calculated for the particle that are regarded as on the interface. Another particle number density n_i^{st1} is calculated at these particles as

$$n_i^{st1} = \sum_{j \neq i} w^{st1}\left(\left|\boldsymbol{r}_j - \boldsymbol{r}_i\right|\right), \tag{15}$$

$$w^{st1}(r) = \begin{cases} 1 & 0 < r \le r_e^{st} \\ 0 & r_e^{st} \le r \end{cases}, \tag{16}$$

Where r_e^{st} is $3.1 l_0$ in this study. The quantity l_0 represents the distance between adjacent particles in the initial particle arrangement. The coefficient 3.1 has not been optimized yet. Accuracy and the computation time should be considered for the optimization.

The particles regarded as on the interface are found in a thickness of d^{st}. In d^{st}, an inside particle has a large n_i^{st1} than that of an outside particle. This lead to errors for the calculation of curvature. The outside particles are identified by smaller particle number densities. Thus, a revised particle number density n_i^{st2} in which the outside particles are excluded is calculated by

$$n_i^{st2} = \sum_{j \neq i} w^{st2}\left(\left|\boldsymbol{r}_j - \boldsymbol{r}_i\right|\right), \tag{17}$$

where

$$w^{st2}(r) = \begin{cases} 1 & 0 < r \le r_e^{st} \text{ and } n_j^{st1} \ge n_j^{st2} \\ 0 & \text{otherwise} \end{cases}. \tag{18}$$

The curvature of the interface is then calculated as

$$2\theta = \frac{n_i^{st2}}{n_0^{st1}}\pi , \tag{19}$$

$$\kappa = \frac{1}{R} = \frac{2\cos\theta}{r_e^{st}} , \tag{20}$$

where n_0^{st1} is constant. This value is calculated where the curvature is zero; the interface is plane.

In this model, curvature of the interface is calculated without drawing the interface. Therefore, a specific algorithm for large deformation of interfaces is not necessary. The unit normal vector is also calculated through particle number density, where the weight function is taken as Eq. (16). The particle number densities at four positions around the particle i are evaluated, $n_i^{\pm x}\left(\boldsymbol{r}_i \pm l_0 \boldsymbol{n}_x\right)$ and $n_i^{\pm y}\left(\boldsymbol{r}_i \pm l_0 \boldsymbol{n}_y\right)$. The unit normal vector to the interface is calculated by

$$\boldsymbol{a}_i = \frac{n_i^{+x} - n_i^{-x}}{2l_0}\boldsymbol{n}_x + \frac{n_i^{+y} - n_i^{-y}}{2l_0}\boldsymbol{n}_y, \tag{21}$$

$$\boldsymbol{n}_i = \frac{\boldsymbol{a}_i}{|\boldsymbol{a}_i|}, \tag{22}$$

Where the vectors $\boldsymbol{n}_x$ and $\boldsymbol{n}_y$ are the unit vectors in the x- and y-direction, respectively.

3. Numerical Analysis of Liquid Droplet Deformation

3.1 Situations

The target situation for the proposed work focuses on the analysis of droplet deformation during the droplet impingement on non-wetted and wetted solid surface. The cases of the target analysis are as follows(Fig. 2),

- Case I. Droplet deformation on the non-wetted solid surface
- Case II. Droplet deformation on the wetted solid surface (shallow water on the solid surface)
- Case III. Droplet deformation on the wetted solid surface (deep water on the solid surface)

The diameter of each droplet is 18 cm. In case II the depth of water pool is 4cm and 8 cm in case III. In case I the initial height of water drop is 14.8 cm and in case II and III initial drop is 10.8 cm above the water initially. Surface tension is 2.361×10^{-2} N/m.

3.2 Results and Discussions

In the calculation water and wall are represented by many particles which are located like a square grid initially. The distance between two neighboring particles l_0 is 8.0×10^{-3} m. The particles on the inner first line of the walls are involved in the pressure calculation. As the source term of the incompressibility model, the particle number densities are needed at these particles. Thus, two other lines of particles should be added outside because r_{en}=2.1 l_0, otherwise the particle number densities are small and the wall particles are recognized as the free surface. In MPS, the wall boundary is represented by arranging fixed particles.

As shown in Fig. 3, water droplet impinges over flat surface and spreads. “With Extreme

viscosity" means that its kinematic viscosity is set to extremely high for the test of viscosity term's robustness. In case of high viscosity spreading speed of droplet is slower than that of "With normal viscosity". Case II and III are shown in Fig. 4 concurrently. In both cases behavior of water is reasonable.

4. Conclusions

Analytical study of water droplet deformation when the droplet impinged onto wetted and non-wetted solid surface is calculated. This analytical work is performed by the Moving Particle Semi-implicit(MPS) method which solves the unsteady Navier-Stokes equations for the liquid droplets. As a result, falling of water droplet on flat surface and shallow/deep water pool was simulated. The present work is, however, limited to an adiabatic process, i.e., no heat transfer between the liquid droplet and solid surface. However, hydrodynamic aspects of the liquid droplet deformation during the impingement are still essential to investigate the subsequent heat transfer during the process.

References

1) S. Koshizuka, Y. Oka, "Moving-Particle Semi-Implicit Method for Fragmentation of Incompressible Fluid," *Nuc. Sci. Eng.*, **123**, 421-434 (1996).
2) Ri-Qiang Duan, Seiichi Koshizuka, Yoshiaki Oka, "Two-Dimensional Simulation of Drop Deformation and Breakup at around the Critical Weber Number," *Nuc. Eng. Design*, **225**, 37-48 (2003).
3) Katsuya Numura, Seiichi Koshizuka, Yoshiaki Oka, Hiriyuki Obata, "Numerical Analysis of Droplet Breakup Behavior Using Particle Method," *J. Nuc. Sci. Tech.*, **38**, 1057-1064 (2001).

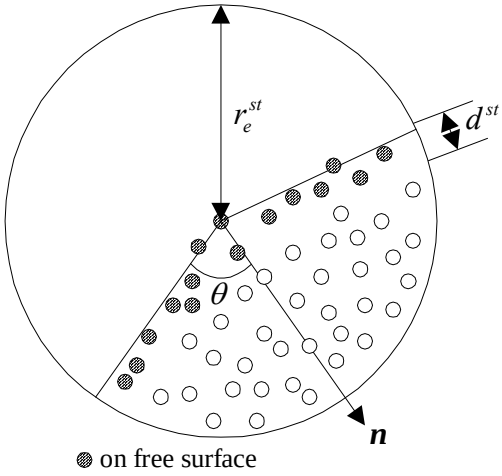

Fig. 1. Surface tension model.

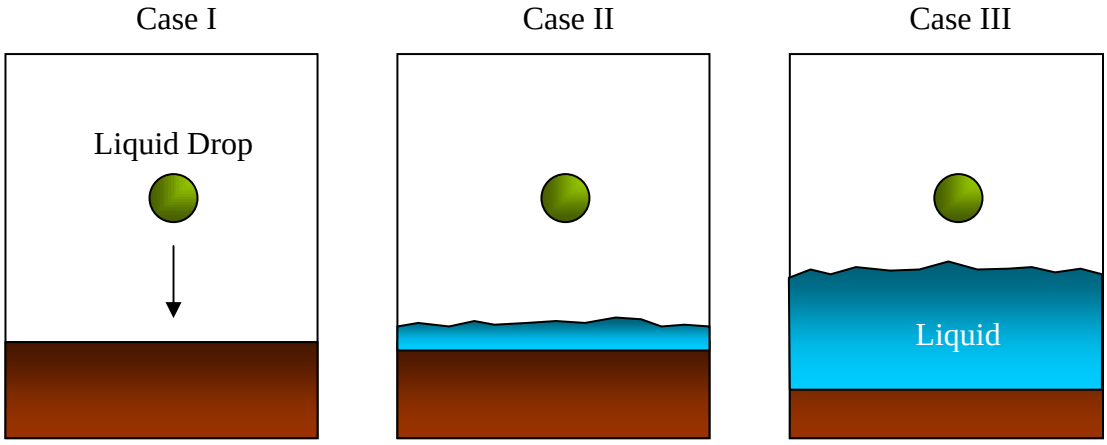

Fig. 2. Target Situations for CFD Analysis

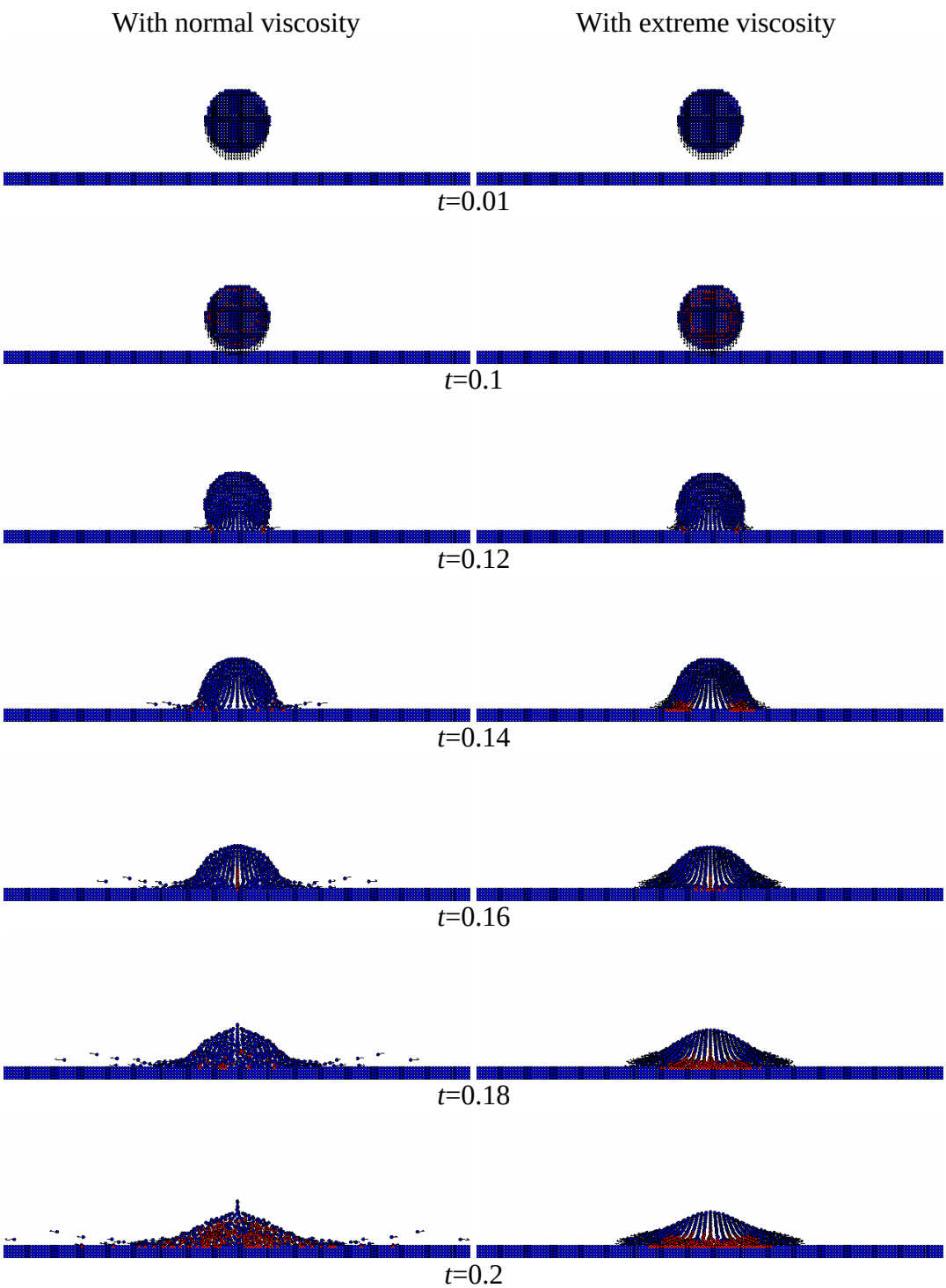

Fig. 3. Droplet deformation on the non-wetted solid surface

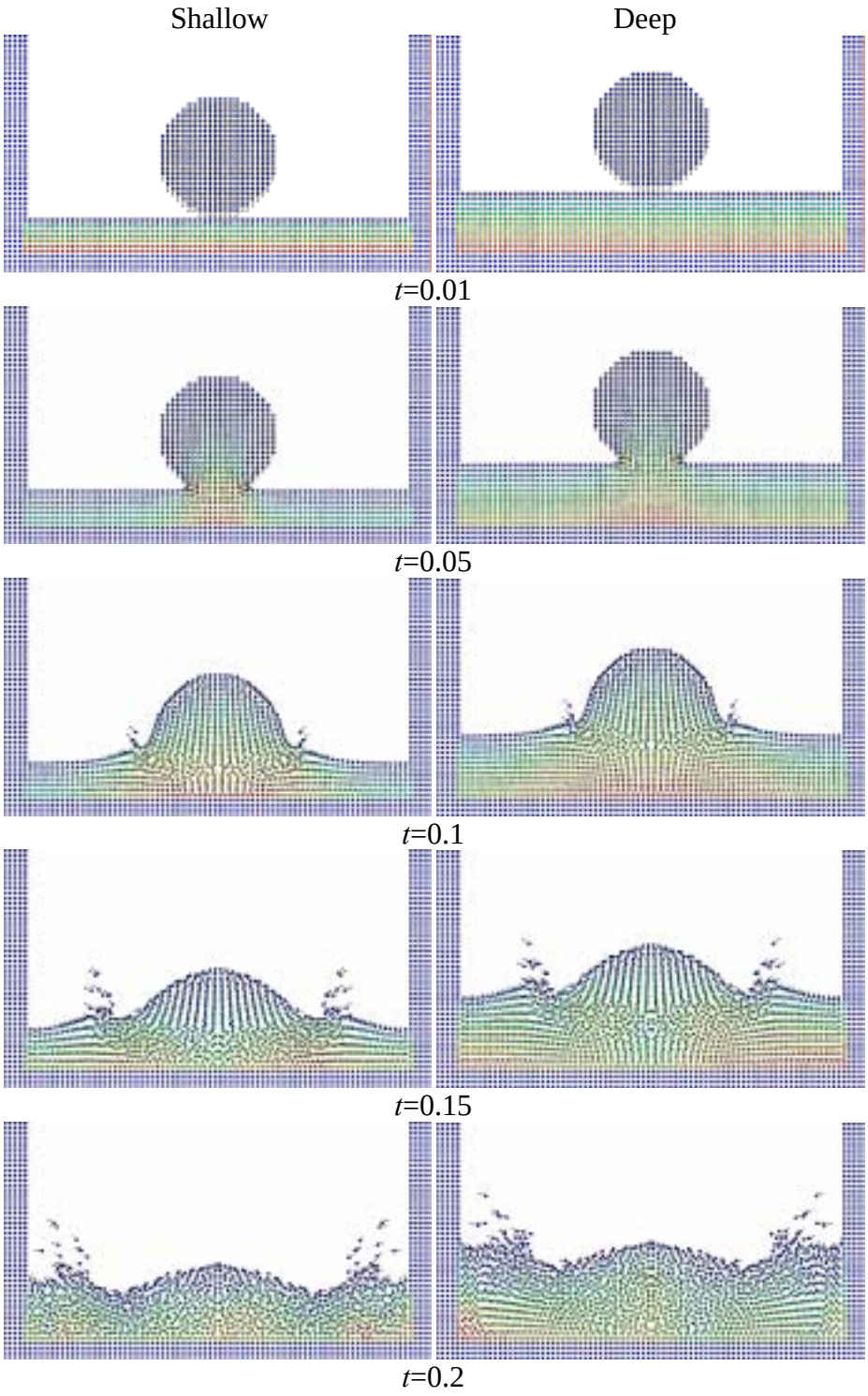
Shallow
Deep
t=0.01
t=0.05
t=0.1
t=0.15
t=0.2

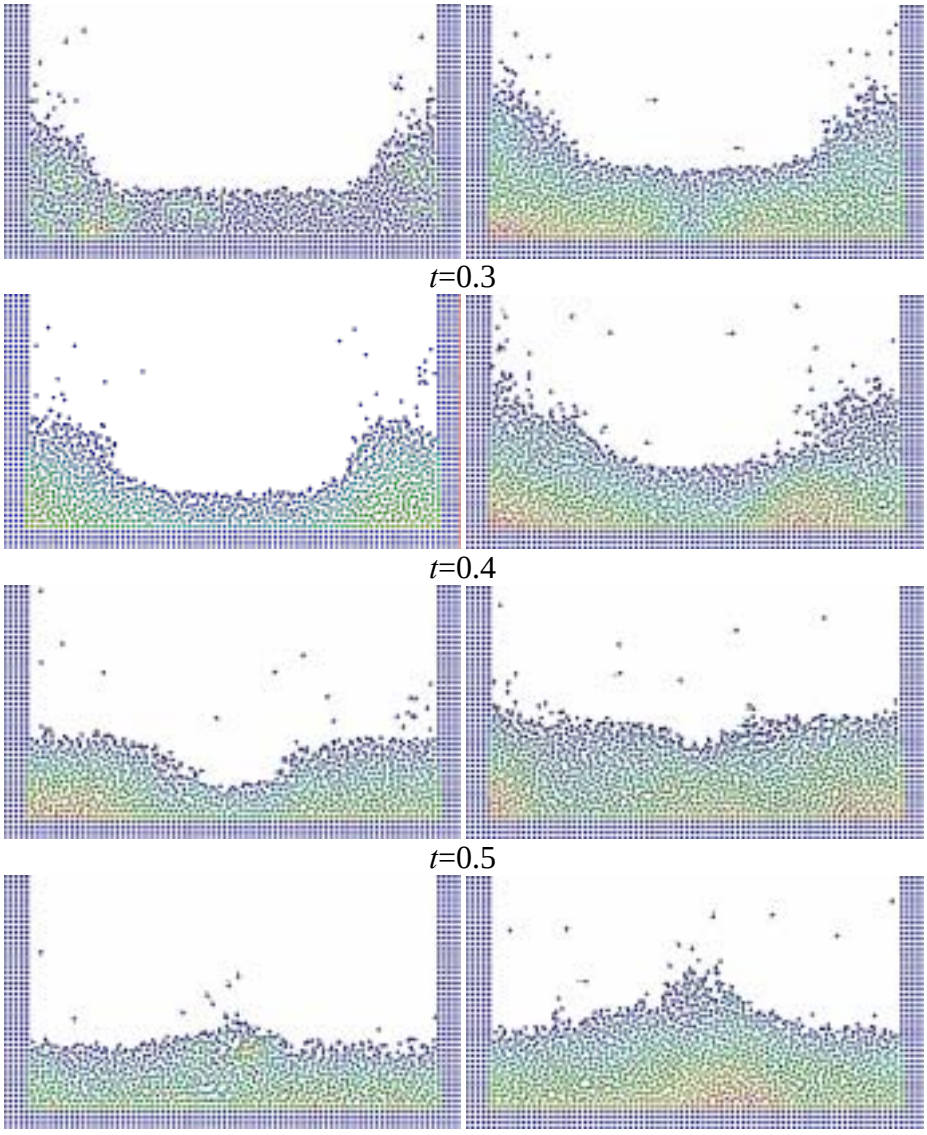

Fig. 4. Droplet deformation on the wetted solid surface
(shallow and deep water on the solid surface)